PHOTO-CONTROLLED PERMEATION OF

SPIROPYRAN MODIFIED GRAMICIDIN A ION CHANNEL

By

Gregory W. Cushing

RECOMMENDED: _Rafail Khairoutdinov_

_____

_____

_____

_____
Advisory Committee Chair

_____
Chair, Department of Chemistry & Biochemistry

APPROVED: _____
Dean, College of Natural Science and Mathematics

_____
Dean of the Graduate School

_April 21, 2006_____
Date

PHOTO-CONTROLLED PERMEATION OF

SPIROPYRAN MODIFIED GRAMICIDIN A ION CHANNEL

A

THESIS

Presented to the Faculty

of the University of Alaska Fairbanks

in Partial Fulfillment of the Requirements

for the Degree of

MASTER OF SCIENCE

By

Gregory W. Cushing, B.S.

Fairbanks, Alaska

May 2006

Abstract

Biomimetic devices show great potential as being molecular sensors of biological species. Gramicidin A (gA) is a well studied ionophore that can be easily modified at the C-terminus to be incorporated into phosphotidylcholine bilayer membrane systems. Potassium permeation of modified gA attached to spiropyran can be controlled with light. Upon ultra-violet irradiation spiropyran transforms to the more polar form merocyanine. The process back to spiropyran is completely reversible upon irradiation with 550 nm light or thermally. Free bilayer membrane vesicles are employed to describe the characteristics of modified ion channels. Characteristics of gA modified with spiropyran are described herein. A device has been created and characterized using electrochemical impedance spectroscopy to analyze potassium permeation through a tethered bilayer membrane system (tBMS) on a sheet of gold utilizing sulfur anchors. The device consists of a tethered phase and a mobile upper phase. The mobile lipid layer incorporates gA modified with spiropyran. The modification allows for control of potassium permeation across the tBMS. Impedance analysis shows good agreement with the ability to control potassium permeation to that of the free vesicle.

Table of Contents

List of Figures

List of Schemes

Chapter 1   Introduction of Biomimetic Systems and Ion Channels

1.1   Introduction to Biomimetic Systems and Historical Examples

Creating technology that mimics nature is nothing new to science. Biomimetics investigates naturally occurring biological processes to provide inspiration for new technological devices. The idea of biomimetics has been around long before the idea became mainstream scientific research. An example of biomimetics thinking is the idea of flying by mimicking the wing of a bird.[1,2] The first literary reference to flight was that of Daedalus.[2] In this ancient flight, wings that resembled the wing of a bird were made of wax. Many years later, the Wright brothers were the first to prove that flight was possible. The shape of the wing was the most important parameter for flight. By mimicking the wing of a bird, ingenuity allowed for the creation of new technology to advance mankind.

1.2   Developing Systems Using a Top-Down or a Bottom-Up Approach

More modern times have allowed for the creation of technology with the help of other technologies. The creation of one device can help the creation of another device. For example, the creation of a machine to make a smaller machine is known as a top-down approach to creating technology. Conversely, a smaller machine can be used to make a larger machine; this is known as a bottom-up approach. Many systems can function as both top-down or bottom-up approaches for building other biological systems.[3-9] The use of individual cells to aggregate together to form a living biological system is an example of a bottom-up approach. One of the most sought after biologically

mimicked systems is the human brain. One must consider which approach to take when dealing with this system. An important question to ask is whether it is more beneficial to create small systems to create a larger system or a larger system to create a smaller system. The former would be an example of today's supercomputers that include smaller units to create one large system. The latter would be an example of making processors smaller and faster to create a smaller system. The mimicking of such complex systems drives scientific research to develop new and innovative materials.

The creation of biological mimicked devices on the scale of a billionth of a meter is known as biomimetic nanotechnology, where nanotechnology refers to technology on the nanometer scale. Materials utilizing such small-scale biological systems include catalysts, solar-power converters, and sensors.[10-13] Catalysts are created by mimicking the active sites of enzymes. Knowing the functional portion of an enzyme makes creating catalysts based on enzyme function a lot easier to produce. The same can be said for reactions involving light conversion to usable energy. Current investigations involve mimicking cellular structure to aid in the conversion of light into usable energy.[10,14,15] Mimicking of cellular structure such as bilayer membrane systems can be developed to act as medium for hosting sensors.

1.3   Using Membrane Systems as a Host for Ion Channels

The membrane system operates as a barrier between the environments on opposing sides of the membrane. Membranes are formed spontaneously by the interaction of lipids aggregating together. The surfactant has two primary regions consisting of a hydrophilic "head group" (attracted to water) and a hydrophobic "tail

group" (water repelling). A bilayer system is formed by the interaction of similar characteristic regions of the surfactant. In an aqueous environment, the hydrophilic head is attracted to the water region while the hydrophobic tail is repelled away from the water region. This interaction with the surfactant and the water environment allow for the spontaneous formation of a bilayer membrane system. Membrane systems are excellent barriers to the transporting of ions. However, transport of ions across membrane systems is very well known to occur in nature and is facilitated by proteins and peptides.[16-19] Such naturally occurring ion transport facilitators include neuronal proteins, halobacterial retinal proteins, and ion-channel forming peptides. Such biological systems facilitate ion diffusion by integrating into the membrane system. In many biologically living systems these proteins/peptides reside within the bilayer membrane of the cell wall.

1.4   Mechanism For Ion Transport Through an Ionophore

Ion diffusion through a bilayer membrane environment can be accomplished in two ways. First, an ionophore can facilitate transport of ions by binding the ion and then diffusing (ion in the ionophore) across the bilayer lipid membrane; valinomycin is such a system.[20] An ionophore is classified as an organic molecule that can facilitate transport of ions across the cell membrane. A second method for ion transport across membranes is by forming a channel within the bilayer membrane, seen in Figure 1.1. Channel proteins and peptides generally have polar interiors that stabilize the ion as it crosses the hydrophobic center of the membrane. The channels often have hydrophobic exteriors that stabilize the channel in the membrane.
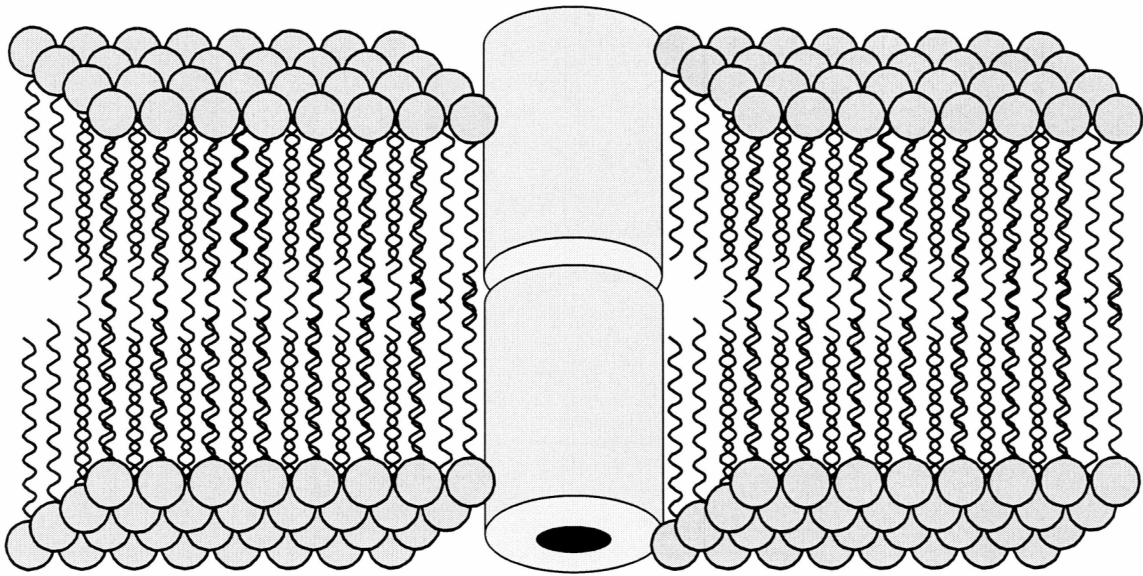
Figure 1.1. Depiction of ion channels integrated into vesicles.

A well studied peptide that forms a channel when incorporated into bilayer membrane systems is gramicidin A. Two individual units of gramicidin A dimerize at the N-termini to form a helical channel through the bilayer membrane. Alternating D and L amino acids of gramicidin A allow for the formation of a helical structure with a 4 Å channel diameter.[21]

The polar side groups of the amino acids turn inward to the core of the channel allowing for the passage of monovalent cations. The outer portion of the channel is non-polar which allows for strong interaction with the hydrophobic region of the bilayer membrane. The opening of the channel is hydrophilic which has an attraction to the bilayer head group. Ion transport can be easily accomplished because of the stabilization the membrane provides for the peptide to form channels.

1.5   Using Chromophores to Probe Local Microenvironment

A photochromic molecule is one that changes color when exposed to light. Some photochromic molecules that have been studied include azobenzenes and spiropyrans. The photoisomerization by which azobenzenes change color is the cis-to-trans transformation induced by irradiation with 430 nm light, as seen in Figure 1.2.[22,23] Exposure to 360 nm ultra-violet light reverses this process. One inherent disadvantage of azobenzenes is that there is very little spectroscopic dependence of the absorption maximum wavelengths (λ_{max}) on the environment's polarity. Therefore, azobenzenes lack the ability to detect change of their local environment by spectroscopic means.
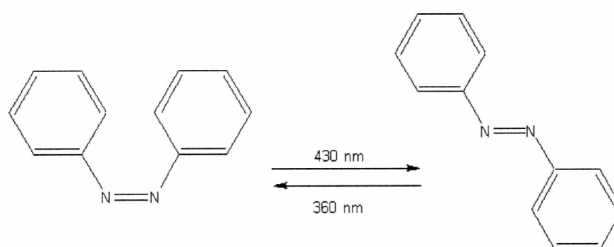
Figure 1.2. Photoisomerization of azobenzenes.

Spiropyran also acts as a photogate molecule. Upon irradiation with 365 nm light, spiropyran transforms into a more polar form, merocyanine.[24,25] This process is reversible by ~550 nm light or heat as seen in Figure 1.3. We have decided to use spiropyrans because noticeable changes in the molecule's spectrum are observed upon changing solvent polarity. Spiropyrans have been previously shown to respond to solvent polarity by shifting the position of the maximum absorption.[26]
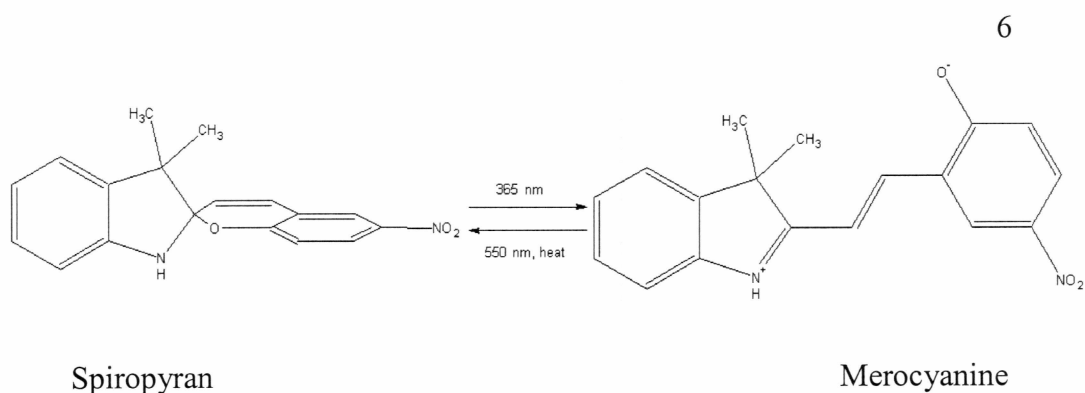
Figure 1.3. Ring opening-closing isomerization reactions of spiropyran to merocyanine.

1.6   Chemically Bonding Spiropyran to Gramicidin A to Control Ion Permeation

Attachment of spiropyran to ion channel proteins has been shown to control ion flux.[27] To control ion transport we have synthesized and studied chemically modified gramicidin A with attached spiropyran (gA-SP). To characterize the functionality of gA-SP, the modified channel is placed into a bilayer membrane system. Studies of the spiropyran location around the channel pore are carried out by time-resolved transient absorption spectroscopy. This experiment is further discussed in chapter 2. Circular dichroism spectroscopy is used to understand peptide backbone structural deformations from attachment of spiropyran to gramicidin A. To visualize spiropyran's location around the peptide pore and the potential to model this system we used the Molecular Mechanics package and the AMBER force field with Hyperchem 7.51. Rates of potassium permeation through the gA-SP channels in free bilayer membrane vesicles are studied using a potassium ion specific probe. These studies demonstrate that we can achieve control over the potassium permeation rate by using light to open or close the ion channel.

1.7   Overview of the Thesis Material

The first chapter has provided an overview of biomimetics and how some of the basic building blocks for technology are designed. The use of photochromic compounds allows control of the biomimetic device. Chapter two is a manuscript submitted for publication in the Journal of the American Chemical Society detailing the characteristics of the spiropyran modified gramicidin A channel within bilayer membrane vesicles. The third chapter entails the construction and characterization by electrochemical impedance spectroscopy of an ion-sensing device incorporating the modified ion channel. The third chapter gives a summary of the work presented in this thesis and provides ideas for future studies.

1.8   References

(1)   Wright, O., Wright, W. *Patent 821,393*. **May 22, 1906**.

(2)   Naso, P. O. *Metamorphoses*; Penguin Books, July 2004.

(3)   Hawker, C. J.; Russell, T. P. *MRS Bulletin* **2005**, *30*, 952.

(4)   Tu Raymond, S.; Tirrell, M. *Adv. Drug Del. Rev.* **2004**, *56*, 1537.

(5)   Wang Kang, L. *J. Nanosci. Nanotechnol.* **2002**, *2*, 235.

(6)   Balzani, V.; Credi, A.; Venturi, M. *Chemistry* **2002**, *8*, 5524.

(7)   Shenhar, R.; Norsten, T. B.; Rotello, V. M. *Intro. Nano. Sci. Tech.* **2004**, 41.

(8)   Zhang, S.; Zhao, X. *J. Mater. Chem.* **2004**, *14*, 2082.

(9)   Zhang, S. *Nat. Biotechnol.* **2003**, *21*, 1171.

(10)   Khairutdinov, R. F.; Hurst, J. K. *Nature* **1999**, *402*, 509.

(11)   Varpness, Z.; Peters, J. W.; Young, M.; Douglas, T. *Nano Letters* **2005**, *5*, 2306.

(12)   Cornell, B. A.; Krishna, G.; Osman, P. D.; Pace, R. D.; Wieczorek, L. *Biochem. Soc. Trans.* **2001**, *29*, 613.

(13)   Cornell, B. A.; Braach-Maksvytis, V. L.; King, L. G.; Osman, P. D.; Raguse, B.; Wieczorek, L.; Pace, R. J. *Nature* **1997**, *387*, 580.

(14)   Ariga, K. *Supramol. Des. Bio. App.* **2002**, 311.

(15)   Tomicki, B. *J. Phys. Chem. B* **2000**, *104*, 1617.

(16)   Kochendoerfer, G. G.; Clayton, D.; Becker, C. *Protein Pept. Lett.* **2005**, *12*, 737.

(17)   Wallace, B. A. *Curr. Top. Mem. Trans.* **1988**, *33*, 35.

(18)   Gliozzi, A.; Robello, M.; Fittabile, L.; Relini, A.; Gambacorta, A. *Biochim. Biophys. Acta* **1996**, *1283*, 1.

(19)   Chattopadhyay, A.; Kelkar, D. A. *J. Biosci.* **2005**, *30*, 147.

(20)   Urry, D. W. *Top. Curr. Chem.* **1985**, *128*, 175.

(21)   Townsley, L. E.; Tucker, W. A.; Sham, S.; Hinton, J. F. *Biochemistry* **2001**, *40*, 11676.

(22)   Bortolus, P.; Monti, S. *J. Phys. Chem.* **1979**, *83*, 648.

(23)   Fischer, E. *J. Am. Chem. Soc.* **1968**, *90*, 796.

(24)   Kalisky, Y.; Orlowski, T. E.; Williams, D. J. *J. Phys. Chem.* **1983**, *87*, 5333.

(25)   Khairutdinov, R. F.; Hurst, J. K. *Langmuir* **2004**, *20*, 1781.

(26)   Pozzo, J. L.; Samat, A.; Guglielmetti, R.; De Keukeleire, D. *J. Chem. Soc., Perkin Trans. 2* **1993**, 1327.

(27)   Kocer, A.; Walko, M.; Meijberg, W.; Feringa, B. L. *Science* **2005**, *309*, 755.

Chapter 2   Photo-Controlled Permeation of Spiropyran Modified Gramicidin A[1]

2.1   Introduction

One focal point in advanced materials research has been the use of supramolecular integrated chemical systems to mimic biological processes. Photoresponsive supramolecular nanoswitches are particularly interesting because they have numerous potential applications to optical sensors, information storage, energy conversion and storage, and optobioelectronic devices.[1-12] Nonetheless, only a few fully light-driven artificial nanoswitches have been reported.[6-9,13-16] In natural photoresponsive proteins, light excitation of a covalently attached chromophore directly changes the protein's activity within a biological membrane. Photoisomerizable molecules such as retinal proteins in halobacteria, open-chain-tetrapyrrole proteins, and xanthopsins represent the basic molecular triggers for many important biological photoreceptors.[17-20] In vision, the first step of the signal transduction in photoreceptors is caused by the structural changes in G-protein induced by a photoexcitation of rhodopsin.[21,22] Activation of the photoreceptor leads to a rapid and transient opening of ion channels in the membrane which results in the production of electrical signals. The common features of natural photoreceptors are: (a) they contain a photochromic molecule attached to a macromolecular protein matrix that spans the bilayer membrane; (b) upon irradiation, the photochromic moiety undergoes reversible stereochemical rearrangements

---

[1] Cushing, G.W. and Khairoutdinov, R.F. 2006. Photo-Controlled Permeation of Spiropyran Modified Gramicidin A. To be published. Department of Chemistry and Biochemistry, University of Alaska Fairbanks, 900 Yukon Drive, Room 194, Box 6160, Fairbanks, AK 99775-6160. E-mail: ffrk@uaf.edu; (907) 474-7654 (voice); (907) 474-5640 (FAX).

between two or more isomeric forms; (c) this primary photochemical reaction induces a conformational change in the attached protein matrix that ultimately leads to a change in the flux of ions across the membrane.

Several approaches have been used to enable light regulation of transmembrane ion transport in artificial systems. Reversible switching of chromophoric compounds doped within the membrane involves one approach to regulating ion diffusion across bilayer membranes.[10,23] Compounds capable of *cis*-to-*trans* photoisomerization have been extensively investigated. The effects of photoisomerization upon ion fluxes have been modest, with the exception of photoreactions that lead to cataclysmic destruction of the membrane.[23-28] Incorporating an ion-binding site into chromophoric compounds capable of photoswitching their position within the membrane was also shown to be a way to control transmembrane ion transport.[29] A light-actuated ionophore consisting of a spiropyran-crown ether supramolecular structure provided transmembrane ion transport with quantum efficiency close to unity before the spontaneous transformation of the optically excited state (MC) to the thermodynamically stable state, spiropyran (SP). The third approach has been to attach a photosensitive gate to natural ion channel proteins.[15,16] There have been several studies on optical control of ion channel gating using photosensitive modified proteins.[9,15,16] Most of these studies employed an azobenzene as the photochromic unit. Although effects of *trans-cis* photoisomerization on channel activity were observed in these cases, a straightforward interpretation of changes in activity was not possible. Utilization of microenvironment-sensitive dyes as photosensing elements would be highly advantageous to developing an understanding of

the basic reaction mechanism.[29] The use of light-activated ion channels could provide

high ion selectivity and extraordinary quantum efficiency of the nanoswitch.

The gramicidin A, gA, channel is the most studied and the best characterized ion-

permeable channel. Gramicidin A is a pentadecapeptide consisting of an altering

sequence of D- and L- amino acids:[30]

HCO-L-Val-Gly-L-Ala-D-Leu-L-Ala-D-Val-L-Val-D-Val-L-Trp-D-Leu-L-Trp-D-Leu-

L-Trp-D-Leu-L-Trp-NHCH$_2$CH$_2$OH

In lipid bilayer membranes, gA adopts a single channel with conformation of a

$\beta^{6,3}$-helical dimer N-terminus to N-terminus structure.[31] This structure is stabilized by

six intermolecular hydrogen bonds, to form a continuous pore through the membrane. In

this conformation, the carboxy terminus of the peptide is exposed to the membrane

interface and the amino terminus is buried in the lipid bilayer. The interior of the channel

is formed by the polar peptide backbone which helps in modulating the channel

conductance. The side chains project outward allowing them to be in contact with

neighboring lipid fatty acyl chains and stabilizing the channel in the bilayer membrane.

In this paper, we describe ion studies of gramicidin ion channels with attached

spiropyran molecules. As shown in our earlier investigations,[10] absorption spectroscopy

allows for the study of the dynamics of photo-induced transformations of these dyes

within the bilayer membrane as well as the controllability of ion permeation. We also

used molecular mechanics calculations to develop a realistic and detailed microscopic picture of photo-controlled ion permeation.

2.2 Experimental Section

2.2.1 Materials

Gramicidin A was purchased from Fluka. 4-(dimethylamino)pyridine, pyridine, and methanol were purchased from Aldrich. Spiropryan carboxylic acid, SP-COOH, was synthesized as reported previously.[32]   N,N'-dicyclohexylcarbodiimide was purchased from Alfa Aesar.

2.2.2 Synthesis of Gramicidin A-Spiropyran

Spiropyran was attached to the *C*-terminus of gA by coupling of spiropyran carboxylic acid directly to the ethanolamine at the C-terminus of gA following a procedure similar to that for a coupling azobenzene dicarboxylic acid to gA reported elsewhere.[9]

Scheme 1. Synthesis of gA-SP.
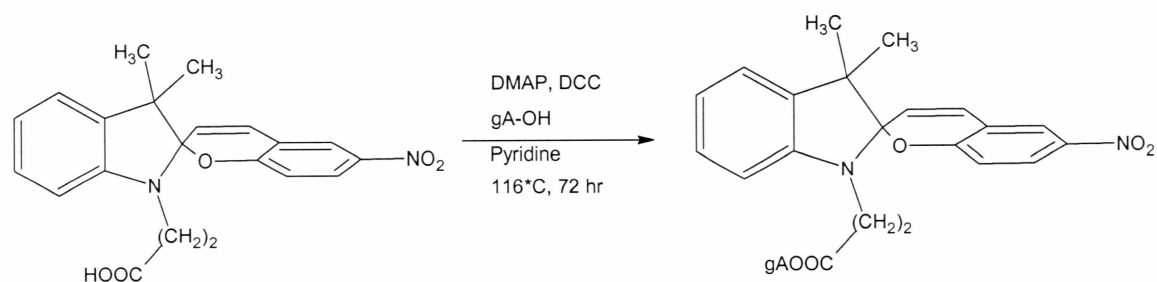
Spiropyran carboxylic acid (28 mg), gramicidin A (50 mg), and 4-(dimethylamino)pyridine (5 mg) were dissolved in 5 mL of dry pyridine and allowed to stir for 15 min under nitrogen. Dicyclohexylcarbodiimide (14.2 μL) was then added and allowed to mix at reflux for 72 hr. The solution was then rotary evaporated to dryness and redissolved in 5 mL of methanol. The solution was subjected to a size-exclusion column using Sephadex LH-20. The recovered solution was dried and a brown solid recovered in 48% yield. The final product was characterized by ^{1}H NMR, UV-VIS, and mass spectrometry. The ^{1}H NMR spectrum was obtained at room temperature using a Varian Mercury 300 MHz FTNMR spectrometer at the frequency 300.068 MHz. NMR (CD_3OD, 300 MHz): (δ 0.28-2.17, m, and 2.69-5.00, m, 86 H; 6.47-7.77, m, ArH, 13 H, 7.96-8.07, m, 1 H, CHO). UV: λ_{max} = 398 nm, log (ε) = 3.4. MALDI-TOF MS: 1883 (gA), 2246 (gA–SP).

2.2.3   Preparation of Vesicles

Egg phosphatidylcholine (PC) was isolated by solvent extraction and chromatography on alumina;[33] the purified product was stored at -10 $^{\circ}$C as a chloroform solution. Unilamellar vesicles with average diameters of 100 nm (PC = 10^{-2} M) were prepared in 20 mM Tris/Cl buffer pH 8.0, from evaporated films by high-pressure extrusion[34] through Isopore Membrane Filters. The relative molar concentration of gA–SP to PC in membrane forming solutions was 1:30, as determined by the weight of materials. Vesicles containing entrapped K^+ were prepared by adding 0.02 M KCl to the buffer prior to extrusion, followed by removal of external potassium ions by size exclusion chromatography using Sephadex G-100. Typically, 5 mL of the vesicle

suspension was applied to a 30×2 cm column and collected in an equal volume of eluent following passage of the void volume. The amount of entrapped K^+ was determined by destroying the vesicles by ultrasonic disruption and measuring the concentration released into the medium using a K^+-specific ion electrode. An average gA-SP/PC molar ratios used in the various experiments was ~500 gA-SP molecules/vesicle.

2.2.4   Physical Measurements

Continuous photolysis experiments were performed using filtered light from a 1.5 kW xenon lamp. The lamp output was focused and passed through aqueous $CuSO_4$ and appropriate glass filters to confine the transmitted light to wavelengths between 340-380 nm (UV) or to > 400 nm (VIS). The filtered light was then passed via an optical fiber bundle to the thermostatted cell. Light intensities were measured using a calibrated PowerMax 500D Laser Power Meter. With the appropriate filters in place, the value was $2×10^{-9}$ einstein/cm^2-s (UV) and $5×10^{-9}$ einstein/cm^2-s (VIS).

The samples were stirred during illumination using a magnetic bar. K^+ release was monitored using an Orion 93-19 K^+-specific and Orion 90-02 counter electrodes connected to an Orion 701A/digital ion analyzer (linear range is 1.0M to 10^{-6} M; the coefficient of variation is 3%).

Optical spectra were recorded using a Hewlett-Packard 8452A diode array instrument interfaced to a ChemStation data acquisition/analysis system.

Transient spectra and kinetics were measured by laser flash photolysis using the third harmonic output (355 nm) from a Continuum Surelite III Nd:YAG laser as the excitation source. Kinetic curves were averages of measurements from at least 10 laser

pulses. Experimental procedures and the instrumental setup have been described in detail elsewhere.[10,24] Ultraviolet Circular Dichroism (CD) spectra were recorded with a Jasco J-720 spectropolarimeter, calibrated by *ammonium d-camphor-10-sulfonate* in a 1 mm quartz cuvette and neodymium glass. An average of three scans were collected with the following parameters: 1 nm bandwidth, 2 s response time, 20 nm/min scan speed, and ambient temperature.[35] Spectra were corrected by subtracting PC vesicles (3.3 mM) in 20 mM Tris/Cl buffer, pH 8.0, as mentioned above.

2.3 Results and Discussion

2.3.1 General Characterization of the System

The spiro carbon atom in spiropyrans effectively blocks transannular π-conjugation between the indoline and pyran rings.[36] Consequently, allowed electronic transitions are relatively high in energy and only appear in the ultraviolet spectral region. Ultraviolet illumination causes the spiropyran (SP) ring of gA–SP conjugate to open, converting it to the merocyanine (MC) form. The merocyanine form of the molecule has a π-bonding network that extends over the entire molecular framework and is more polar (Scheme 2).

Scheme 2. Ring Opening-Closing Isomerization Reactions of gA–SP.
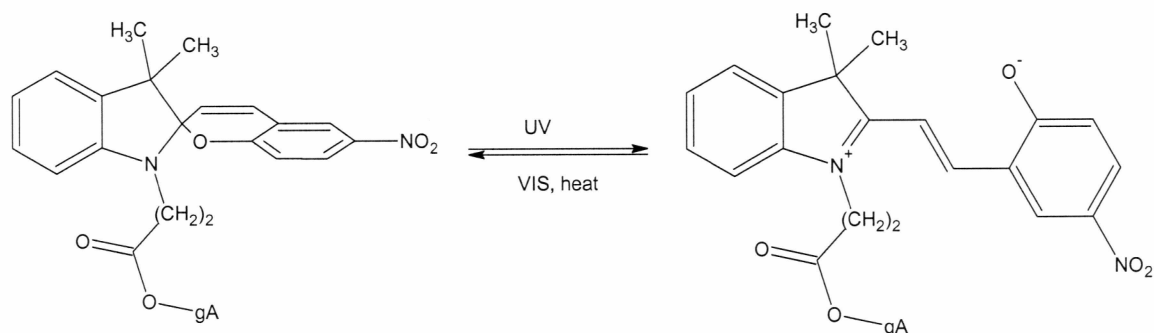
One manifestation of this increased electronic delocalization is that allowed transitions now appear in the visible spectral region. The ring opening reaction can be reversed by illumination in the visible band, or via a thermal reaction.

The nature of the optical changes that occur is illustrated for gA–SP in PC liposomes in Figure 2.1 (*left panel*), where the spectra obtained under UV and VIS illumination are compared. The λ_{max} is defined by subtracting the spiropyran absorption profile from the merocyanine absorption profile in the visible region. It is observed that when using organic solvents the position of the visible band is solvent-sensitive, shifting λ_{max} to higher energies as the polarity increased (Figure 2.1, *right panel*). This behavior is typical for spiropyrans and has been explained as arising from a reduced polarity of the electronic excited state in the merocyanine form of the dye.[37]

Solvent dependence of the position of the visible band for related a $C_{15}H_{31}COO-$ MC compound is also shown in Figure 2.1 (*right panel*).[29] The solvent polarity affects the position of the visible band of gA–MC much more weakly than that of $C_{15}H_{31}COO-$ MC. The two sets of data intersect at $\epsilon\sim15$. This observation indicates that the interaction of merocyanine with the polar C-terminus of gA is comparable with the

interaction of merocyanine with a solvent with $\varepsilon \approx 15$. The combined interaction of MC

with the polar C-terminus of gA and with solvent molecules decreases the effect of the

solvent on the position of the visible absorption maximum of gA–MC in comparison with

that of $C_{15}H_{31}COO$–MC.

The visible band maxima of the gA–MC obtained in PC vesicles (~555 nm)

during continuous illumination with UV light were comparable to the wavelength

maxima measured in polar solvents, that is, with an effective $\varepsilon > 30$, consistent with

localization of the dyes within the polar headgroup region of membrane.[24,39-41]
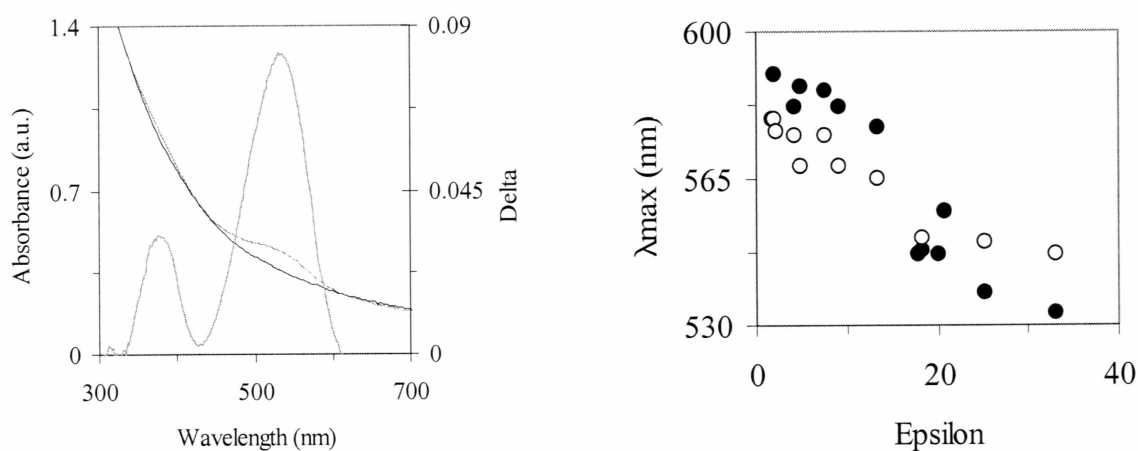
Figure 2.1. *Left panel.* Absorption spectrum of gA–SP in PC vesicles (red) and gA-

MC(black). The difference in absorption spectra is shown in green. *Right panel.*

Dependence of λmax for gA–MC (open circles) and C15H31COO–MC (closed circles)[29]

on solvent dielectric constant (ϵ). Solvents used (ϵ in parentheses) were pentane (1.84),

cyclohexane (2.02), dioxane (2.22), diethyl ether (4.27), chloroform (4.81),

tetrahydrofuran (7.52), dichloromethane (9.08), pyridine (13.3), 1-butanol (17.8), 2-

propanol (20.2), 1-propanol (20.8), , ethanol (25.3), methanol (33.0).[38]

2.3.2   Time Resolved Measurements

The visible absorption bands of transient spectra recorded immediately following

355 nm laser pulse excitation were red-shifted relative to their steady-state positions

(Figure 2.2, *left panel*). These changes in transient spectra were manifested in temporal

increases in absorbance at wavelengths longer than the steady-state maximum with

symmetric decreases at shorter wavelengths. The decay could be fitted at all wavelengths

to a simple first-order relaxation profile whose lifetime was 58 ms (Figure 2.2, *right*

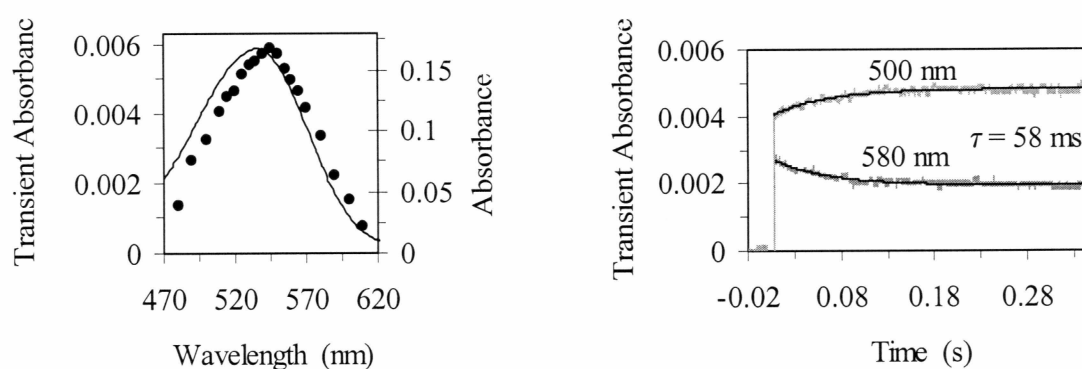*panel*).

Figure 2.2. *Left panel*. Absorption spectra of PC liposome containing gA-SP after

continuous illumination (line) and 1 ms after a 355 nm laser pulse (solid circles). *Right*

panel. Normalized relaxation kinetics at 500 and 580 nm of the transient absorption of

gA-SP doped PC vesicles. The solid lines are the exponential best fit decay curves

obtained with $\tau = 58$ ms.

This behavior is very similar to that found for simple photochromic spiro compounds, whose photoisomerization reactions in solution occur on subpicosecond time scales[42-44] and for which the slow secondary relaxation is observed only when the compounds are incorporated within vesicles.[10,24] Thus, it appears that rapid gA–SP → gA–MC photoisomerization is followed by a structural reorganization ($\tau = 58$ ms) in which the environment of the dye becomes more polar.

The slow relaxation step was also observed when photoisomerization of the gA–SP was carried out in homogeneous solution. However, the visible transient absorption bands were red-shifted relative to their equilibrium positions only in solvents with $\varepsilon > 15$. They were blue-shifted in solvents with $\varepsilon < 15$ corresponding to a decrease in the transient absorbance at 590 nm, which is above λ_{max} in methanol, ($\varepsilon = 33.0$) and an increase in chloroform ($\varepsilon = 4.81$), shown in Figure 2.3. The data indicate that fast gA–SP → gA–MC photoisomerization in solutions is followed by a slow structural rearrangement. The result is a relocation of MC from a position more open to solvent molecules to a position where MC interacts more strongly with the C-terminus of gramicidin A. In order to confirm this conclusion we investigated this relocation by molecular dynamics (MD) simulations with the AMBER force field of the structures gA–SP and gA–MC dimers.
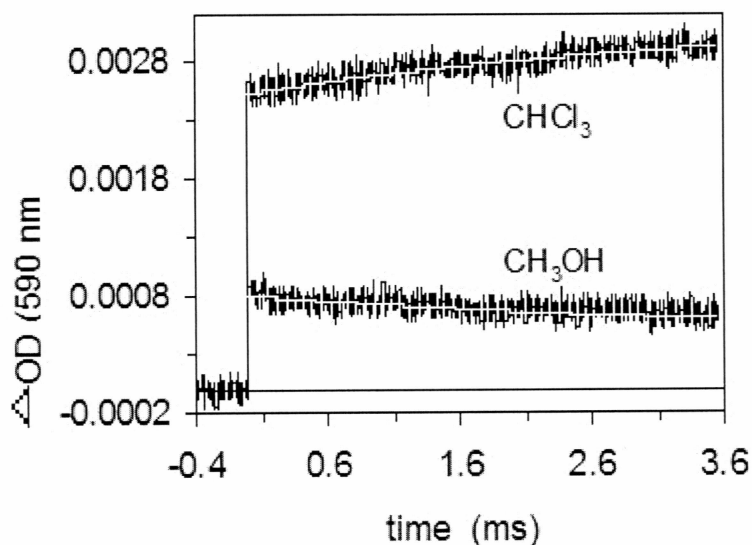
Figure 2.3. Decay kinetics of the 355 nm laser pulse-induced transient absorption at 590 nm for gA–SP in methanol and chloroform. Conditions are kept the same as in Figure 2.2. The smooth lines are the exponential fits of the relaxation steps, for which $\tau \approx 4$ ms.

2.3.3   Molecular Dynamics Simulations

The small size but regular and stable structure of gramicidin A makes it ideal for molecular dynamic (MD) simulations. Models of gA–SP and gA–MC were then built using the NMR derived membrane-bound structure of gramicidin A (Protein Data Bank Code 1JNO) as a starting point.[45] For the molecular dynamics simulations, the AMBER force field package was used.[46] Within this package, harmonic constraints are employed to represent the covalent bonds among the peptide atoms and the nonbonded interactions are represented in terms of the pairwise Coulomb and Lennard-Jones interactions. Despite its simplicity and neglect of polarization effects, this package has been quite successful in description of protein complexes.

Determination of the torsion angle in the gA-SP molecule at the ethanolamine portion with the lowest energy was found using the Hyperchem 7.51 *conformational search* option with the Molecular Mechanics *AMBER* force field.[47] The torsion angle was given no restrictions to movement. The lowest energy torsion angle was found to be -76.5° for gA-SP and 177.0° for gA-MC.

MD simulations in vacuum place spiropyran close to the less polar region of gA or the outside of the peptide, whereas, optimizations position merocyanine towards the channel pore of gA (Figure 2.4). Calculations show that in vacuum merocyanines impede ion access to the gA channel while spiropyrans leave the entrance of the channel practically intact.
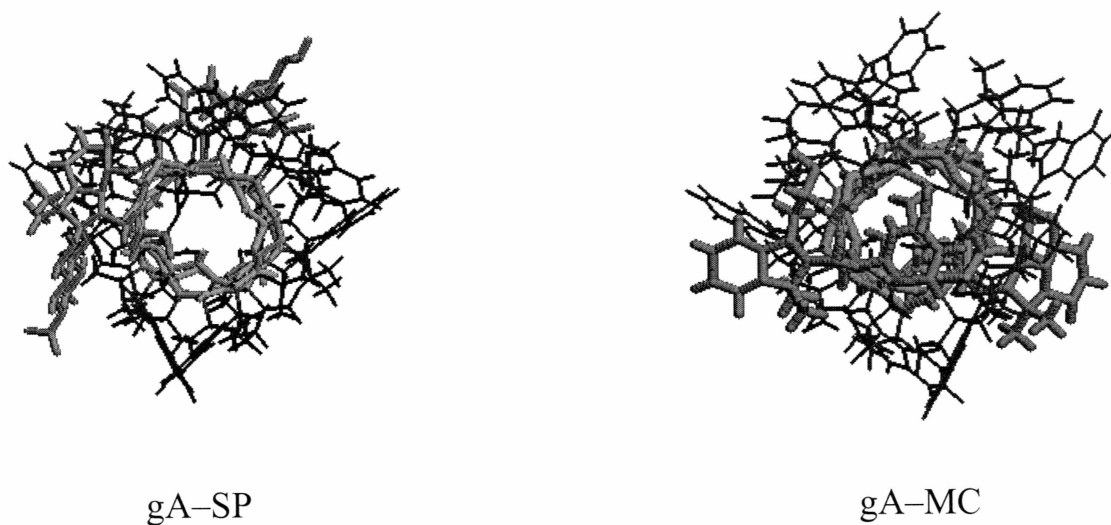

gA–SP   gA–MC

Figure 2.4. Optimized structures of gA–SP and gA–MC ion channels in vacuum. The polar peptide backbone is shown in green, hydrophobic side chains are shown in black, and attached SP and MC are shown in red.

2.3.4   Potassium Ion Release Study

To investigate potassium leakage rates through vesicles we compared K^+ thermal leak rates of gA-SP to gA mixed with SP in vesicles. The thermal leak rate of 20 mM entrapped K^+ from PC vesicles is ~1.2 nM/s. The addition of 40 μM gA into the 80 nM PC vesicles increased the initial leak rate to ~16 nM/s (see Figure 2.5, *left panel*). The leak rate remained unchanged upon further addition of 40 μM SP to the membrane. Switching between UV/Vis illumination of the gA + SP containing vesicles is not observed to affect K^+ leakage. The thermal leak rate of entrapped K^+ ions from PC vesicles containing just SP changed from ~ 0.3 nM/s under visible light illumination to ~ 0.1 nM/s under UV illumination. These changes are presumably due to light induced reversible SP↔MC transformations that translocate spiropyran in the PC membrane and modulate the leak rate of K^+ ions.

We presume the mechanism by which gA allows for leakage of K^+ through the channel is the same for gA-SP. The thermal leakage of K^+ with modified gA–SP containing PC vesicle membrane under visible illumination is significantly slower, ~4.8 nM/s (see Figure 2.5, *right panel*). UV illumination of the gA–SP vesicle suspension caused the ion leak rate to decrease to ~2.4 nM/s, approximately a 50% decrease in K^+ leakage.
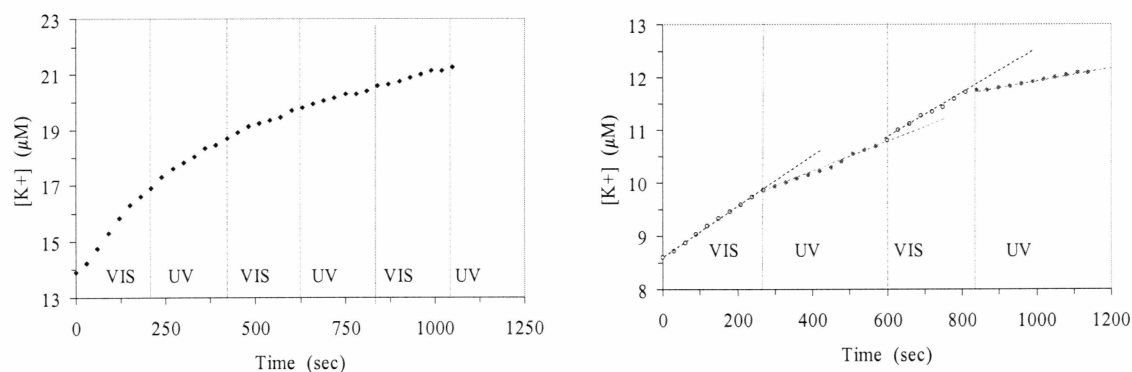
Figure 2.5. Release of K^+ from 89 nM PC vesicles accompanying reversible SP↔MC photocycling. *Left panel*: PC vesicles containing gA (40 µM) + SP (40 µM). *Right panel*: PC vesicles containing gA–SP (40 µM). The vertical lines divide intervals where suspensions were exposed to VIS or UV illumination. The open circles are data points; the dashed lines are linear fits of the corresponding kinetics of K^+ release.

2.3.5   Circular Dichroism Study

Gramicidin A exhibits positive ellipticities at 215 and 235 nm. A modified gramicidin A should demonstrate circular dichroism ellipticities similar to that of unmodified gramicidin A if the helical structure is kept intact. Figure 2.6 shows the ellipticity of native gramicidin A, gramicidin A mixed with spiropyran/merocyanine, and gA-SP/MC. Very little difference in ellipticity is noticed between the spiropyran and merocyranine forms of both modified gramicidin A and gramicidin A mixed. Positive ellipticity is observed at both 215 and 235 nm for modified gramicidin A indicating helical structure is kept intact upon attachment of spiropyran to gramicidin A.
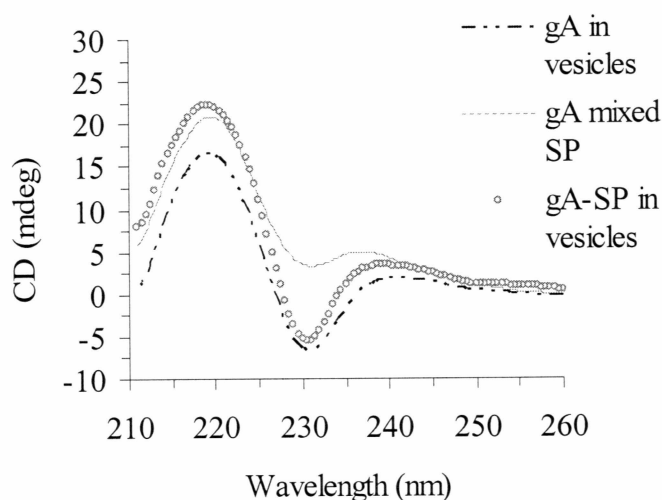
Figure 2.6. Circular dichroism of gramicidin A, gA mixed with spiropyran, and gA-SP.

2.4   Conclusion

Demonstrated here is the ability to control potassium ion flow by means of

photoregulating spiropyran attached to gramicidin A. Studies indicated that spiropyran

interacts more strongly with the polarities of gramicidin A rather than that of the

surrounding microenvironment. Computer optimization calculations using the AMBER

force field method predict placement of spiropyran in coordination to gramicidin A

giving insight into studies. Circular dichroism measurements indicate that channel

structure of modified gramicidin A with spiropyran remains similar to that of unmodified

gramicidin A in PC vesicles. K^+ permeability of gA-SP can be controlled by irradiation

with either ultra-violet or visible light with a 100% increase in K^+ permeation from the

"closed" to the "opened" states. We have shown here the chemical modification and

manipulation of gramicidin A with spiropyran.

2.5   Acknowledgements

2.6   References

(1)   Willner, I.; Katz, E.; Willner, B.; Blonder, R.; Heleg-Shabtai, V.; Buckmann, A. F. *Biosens. Bioelectron.* **1997**, *12*, 337.

(2)   Khairutdinov, R. F.; Hurst, J. K. *Nature* **1999**, *402*, 509.

(3)   Lucchesi, L. D.; Khairutdinov, R. F.; Hurst, J. K. *Colloids Surf., A* **2000**, *169*, 329.

(4)   Khairutdinov, R. F.; Hurst, J. K. *J. Am. Chem. Soc.* **2001**, *123*, 7352.

(5)   Cattrall, R. W. *Chemical Sensors*; Oxford University Press: Oxford, 1997.

(6)   Lehn, J. M. *Supramolecular Chemistry: Concepts and Perspectives*; John Wiley & Son Ltd: N.Y., 1995.

(7)   Gobbi, L.; Seiler, P.; Diederich, F.; Gramlich, V. *Helv. Chim. Acta* **2000**, *83*, 1711.

(8)   Borisenko, V.; Burns, D. C.; Zhang, Z.; Woolley, G. A. *J. Am. Chem. Soc.* **2000**, *122*, 6364.

(9)   Osman, P.; Martin, S.; Milojevic, D.; Tansey, C.; Separovic, F. *Langmuir* **1998**, *14*, 4238.

(10)   Khairutdinov, R. F.; Hurst, J. K. *Langmuir* **2001**, *17*, 6881.

(11)   Shishido, A.; Tsutsumi, O.; Kanazawa, A.; Shiono, T.; Ikeda, T.; Tamai, N. *J. Am. Chem. Soc.* **1997**, *119*, 7791.

(12)   Ikeda, T.; Sasaki, T.; Ichimura, K. *Nature* **1993**, *361*, 428.

(13)   Willner, I.; Willner, B. *Biotechnol. Progr.* **1999**, *15*, 991.

(14)   Willner, I. *Acc. Chem. Res.* **1997**, *30*, 347.

(15)   Banghart, M.; Borges, K.; Isacoff, E.; Trauner, D.; Kramer, R. H. *Nat. Neuro.* **2004**, *7*, 1381.

(16)   Kocer, A.; Walko, M.; Meijberg, W.; Feringa, B. L. *Science* **2005**, *309*, 755.

(17)   Kort, R.; Hoff, W. D.; Van West, M.; Kroon, A. R.; Hoffer, S. M.; Vlieg, K. H.; Crielaard, W.; Van Beeumen, J. J.; Hellingwerf, K. J. *EMBO J.* **1996**, *15*, 3209.

(18)   Oesterhelt, D. *Biochem. Int.* **1989**, *18*, 673.

(19)   Ramos-Boudreau, C.; Cobley, J.; Tandreau de Marsac, N. *Book of Abstracts, 219th ACS National Meeting, San Francisco, CA, March 26-30,* **2000**, BIOL.

(20)   R. M. Williams, S. B. Triggering of Photomovements - Molecular Basis. In *Photomovement*; Haeder, D. P. L., M. Eds., Ed.; Elsevier: Amsterdam, 2001; pp 15.

(21)   Natochin, M.; Moussaif, M.; Artemyev, N. O. *J. Neurochem.* **2001**, *77*, 202.

(22)   Baylor, D. *Proc. Natl. Acad. Sci. U. S. A.* **1996**, *93*, 560.

(23)   Weh, K.; Noack, M.; Ruhmann, R.; Hoffmann, K.; Toussaint, P. *Chem. Ing. Tech.* **1998**, *70*, 718.

(24)   Khairutdinov, R. F.; Giertz, K.; Hurst, J. K.; Voloshina, E. N.; Voloshin, N. A.; Minkin, V. I. *Journal of the American Chemical Society* **1998**, *120*, 12707.

(25)   Morgan, C. G.; Thomas, E. W.; Sandhu, S. S.; Yianni, Y. P.; Mitchell, A. C. *Biochim. Biophys. Acta, Biomem.* **1987**, *903*, 504.

(26)   Song, X.; Perlstein, J.; Whitten, D. G. *J. Am. Chem. Soc.* **1997**, *119*, 9144.

(27)   Aoyama, M.; Watanabe, J.; Inoue, S. *J. Am. Chem. Soc.* **1990**, *112*, 5542.

(28)   Lei, Y.; Hurst, J. K. *Langmuir* **1999**, *15*, 3424.

(29)   Khairutdinov, R. F.; Hurst, J. K. *Langmuir* **2004**, *20*, 1781.

(30)   Sarges, R.; Witkop, B. *J. Am. Chem. Soc.* **1965**, *87*, 2011.

(31)   Allen, T. W.; Andersen, O. S.; Roux, B. *J. Am. Chem. Soc.* **2003**, *125*, 9868.

(32)   Hirakura, T.; Nomura, Y.; Aoyama, Y.; Akiyoshi, K. *Biomacromolecules* **2004**, *5*, 1804.

(33)   Nielsen, J. R. *Lipids* **1980**, *15*, 481.

(34)   Hope, M. J.; Nayar, R.; Mayer, L. D.; Cullis, P. R. *Liposome Technol. (2nd Ed.)* **1993**, *1*, 123.

(35)   Shobini, J.; Mishra, A. K.; Chandra, N. *J. Photochem. Photobiol., B* **2003**, *70*, 117.

(36)   J. C. Crano, R. J. G., Eds. *Organic Photochromic and Thermochromic Compounds*; Plenum Press: New York, 1999; Vol. 1.

(37)   Pozzo, J. L.; Samat, A.; Guglielmetti, R.; De Keukeleire, D. *J. Chem. Soc., Perkin Trans. 2* **1993**, 1327.

(38)   Lide, D. R. *CRC Handbook of Chemistry and Physics, 83rd Edition*, 2002.

(39)   Wiener, M. C.; White, S. H. *Biophys. J.* **1992**, *61*, 434.

(40)   Sanders, C. R., II; Schwonek, J. P. *Biophys. J.* **1993**, *65*, 1207.

(41)   Mazeres, S.; Schram, V.; Tocanne, J.-F.; Lopez, A. *Biophys. J.* **1996**, *71*, 327.

(42)   Zhang, J. Z.; Schwartz, B. J.; King, J. C.; Harris, C. B. *J. Am. Chem. Soc.* **1992**, *114*, 10921.

(43)   Wilkinson, F.; Worrall, D. R.; Hobley, J.; Jansen, L.; Williams, S. L.; Langley, A. J.; Matousek, P. *J. Chem. Soc., Faraday Trans.* **1996**, *92*, 1331.

(44)   Tamai, N.; Masuhara, H. *Chem. Phys. Lett.* **1992**, *191*, 189.

(45)   Townsley, L. E.; Tucker, W. A.; Sham, S.; Hinton, J. F. *Biochemistry* **2001**, *40*, 11676.

(46)   Weiner, S. J.; Kollman, P. A.; Case, D. A.; Singh, U. C.; Ghio, C.; Alagona, G.; Profeta, S., Jr.; Weiner, P. *J. Am. Chem. Soc.* **1984**, *106*, 765.

(47)   HyperChem(TM) Professional 7.51, H., Inc., 1115 NW 4th Street, Gainesville, Florida 32601, USA.

Chapter 3   Conclusion and Future Studies of Spiropyran Modified Gramicidin A

3.1   Conclusions of the Spiropyran Modified Gramicidin A Channel

In Chapter 2, the modification of gramicidin A with a microenvironment-sensitive chromophore such as spiropyran was demonstrated to control potassium permeation across a bilayer membrane. The absorbance of spiropyran exhibits a shifting to higher energies when solvent polarity increases, known as a hypsochromic shift. Transient absorption kinetic studies were accomplished by comparing the effects of gramicidin A-spiropryan incorporated into vesicles to that of gramicidin A-spiropyran in high and low dielectric solvents. When exposed to a high energy pulse of light (355nm) the transient absorption of λ_{max} of gA-SP is observed to decrease in polar solvents and increase in non-polar solvents. This indicates that the transformation of spiropyran to merocyanine is shifting from a polar to a more non-polar microenvironment. Computational modeling *in vacuo* has predicted that spiropyran resides close to the non-polar outside of the channel pore, whereas merocyanine is placed near the polar pore-opening. Potassium ion permeation is observed to increase 100% when the chromophore is converted from merocyanine to spiropyran. The reversibility of this conversion process is shown in Figure 3.1.
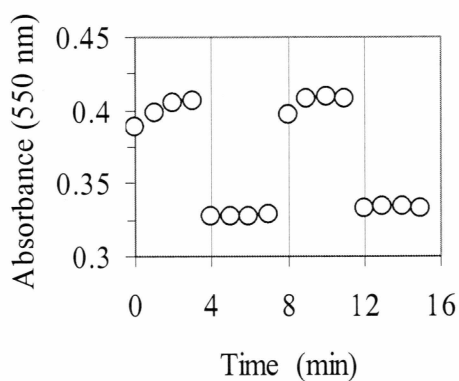
Figure 3.1. Absorbance measured at 550 nm of gA-SP in vesicles of alternating cycles of UV and VIS light.

Circular dichroism was used to determine the amount of deformation of the peptide backbone of the gramicidin A channel upon modification with spiropyran. The helicity of gA-SP is similar to that of gA in phosphatidylcholine vesicles indicating the channel is still present upon addition of spiropyran.

3.2   Future Studies

To study further the kinetics of K^+ ion transport, impedance spectroscopy may be used.[1,2] The ion channel will be incorporated into a system of synthetic lipids tethered to a gold sheet acting as a working electrode, Figure 3.2.[3-6]
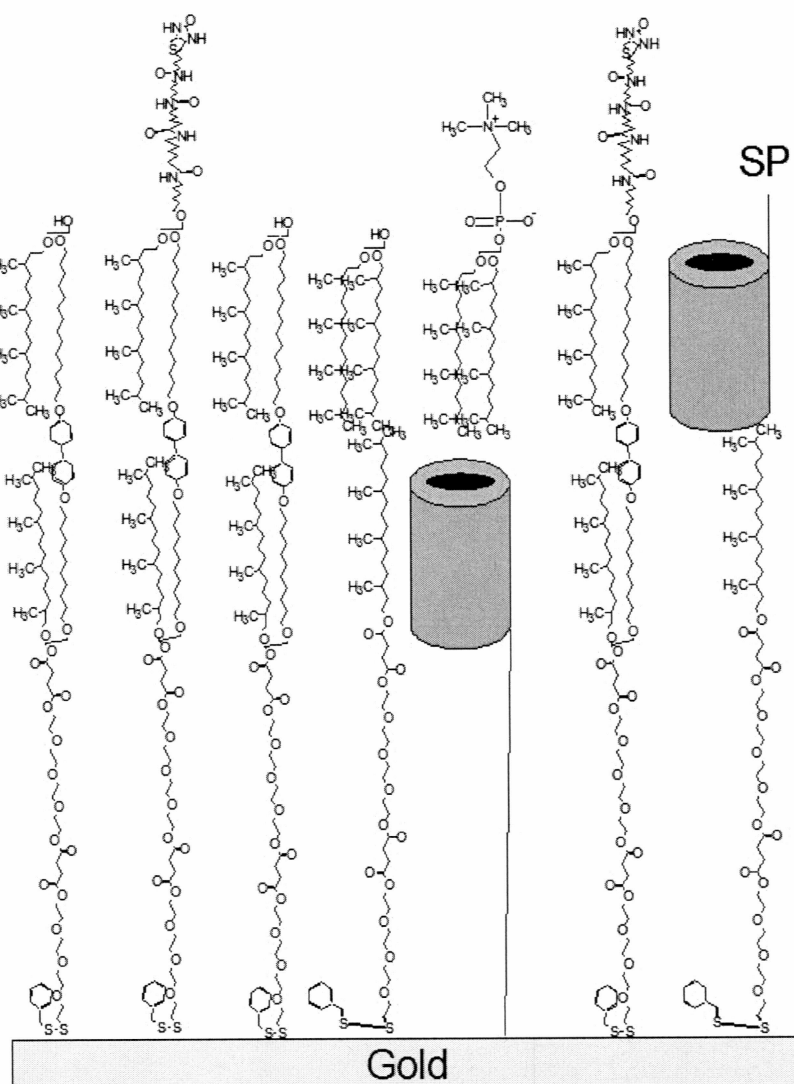
Figure 3.2. A cartoon representation of the tethered system incorporating gA-SP.

To characterize the channel conductance a simple equivalent circuit model can be used to describe the membrane incorporating gA-SP. The equivalent circuit model can be seen in Figure 3.3. A simple model is used to describe the membrane system by evaluating the membrane system as an alternating current circuit. The use of complicated models to describe the membrane can lead to misrepresentation of the overall system.
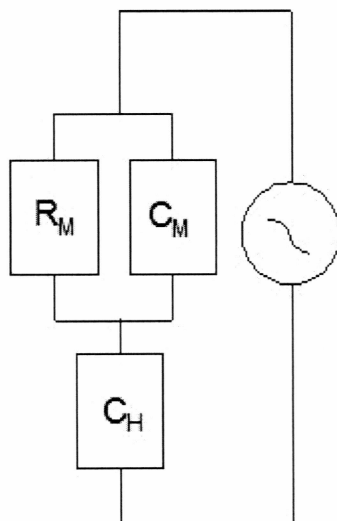
Figure 3.3. The equivalent circuit diagram of gA-SP incorporated into a synthetic lipid system.

The membrane capacitance and resistance is described by C_M and R_M, respectively. The Helmholtz capacitance (C_H) describes the double-layer capacitance of the electrode with an electrolyte solution. Figure 3.4 further describes the Helmholtz double-layer capacitance in a cartoon illustration. A typical value of C_M/area is ~0.5 $\mu S/cm^2$ and for C_H/area is ~5.0 $\mu S/cm^2$. The total capacitance of the system can be described as $C = (C_H C_M)/(C_H + C_M)$. The total capacitance has <10% contribution from C_H so that the C $\approx C_M$. The channel conductance is equivalent (at low frequencies) to $1/R_M$.[6]
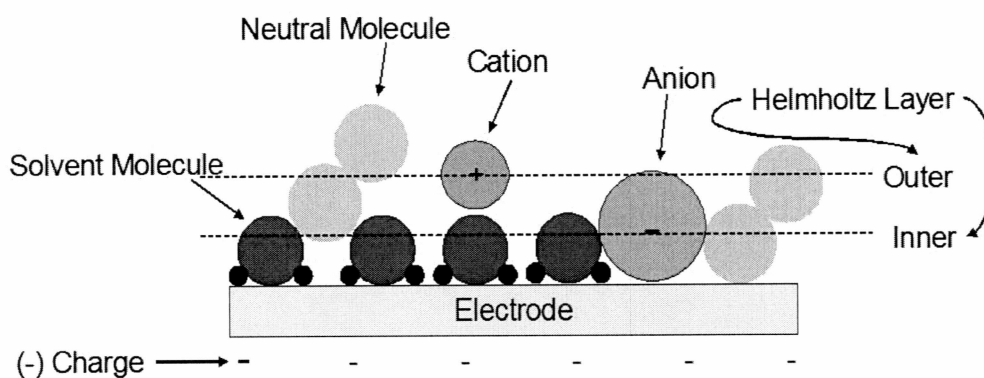
Figure 3.4. Cartoon illustration of the Helmholtz double-layer.

The importance of this study will be to determine the conductance of ions through the spiropyran modified gramicidin A channel. The two conformations of the "open" and "closed" form of the gA-SP channel will be apparent through the conductance of ions at specified electrolyte concentrations. The importance of this information will be to determine the kinetics of ion transport across the gramicidin A channel. Channel characteristics of gramicidin A have been previously studied and incorporated into a tethered lipid system. The use of proper lipids to describe channel conductance has been thoroughly investigated.[1-5]

3.3   Impedance Measurements

The impedance spectrum can be obtained by sweeping an applied 50 mV ac potential from 1 to 1000 Hz superimposed onto a 300 mV dc offset. A three electrode excitation is used with a gold working electrode, platinum counter electrode, and a silver/silver chloride reference electrode. Data will be obtained by applying a simple equivalent circuit as described elsewere using the Gamry Echem Analyst software.[6]

Measurements are made in a series of electrolyte solutions of KCl with varying concentrations from 1, 50, 100, to 500 mM.

3.4   Membrane Preparation

All membrane components, unless otherwise stated, can be purchased from Ambri Lt. Spiropyran modified gramicidin A will be made as described in chapter 2. Slides coated with 1000 Å gold on top of a titanium adhesion layer can be purchased from Sigma-Aldrich. Milli-Q water must be freshly collected before each use. All data will be recorded on a Gamry Ref600 Impedance Spectrometer.

The gold coated slides should be submerged in a solution of the tethered membrane layer dissolved in ethanol for 72 hours. Slides can be stored at 4°C until tested by rinsing thoroughly with ethanol. The mobile outer layer should be prepared from a 3 mM solution of a lipid solution purchased from Ambri Limited and 37.5 nM gA-SP in ethanol. The gold slide prepared with the tethered layer is fastened to an ultra-high molecular weight polyethylene well. The approximate well area has been designed to 0.317 cm^2 with a well volume of 250 μL. Approximately 28.5 μL of mobile solution will be injected into the well following by 100 μL of water and allowed to incubate for 10 minutes. The well is then washed thoroughly with water and replaced with the KCl solution.

3.5   Importance of Controlling Ion Permeation

The uses of microphase-organized integrated chemical systems to accomplish specific tasks are envisioned, but largely unrealized. Many applications such as

electronics, sensors, and biomedicines require molecular switches. These switches can be accomplished by electronic, ionic, chemical, or photonic stimulation. With a deeper understanding of just how to functionalize switching materials, development of advanced materials to accomplish specific tasks can be achieved. Studying and modifying the most characterized ion channel known allows for a greater understanding of how to begin developing advanced materials.

3.6   References

(1)   Cornell, B. A.; Braach-Maksvytis, V. L.; King, L. G.; Osman, P. D.; Raguse, B.; Wieczorek, L.; Pace, R. J. *Nature* **1997**, *387*, 580.

(2)   Cornell, B. A.; Krishna, G.; Osman, P. D.; Pace, R. D.; Wieczorek, L. *Biochem. Soc. Trans.* **2001**, *29*, 613.

(3)   Krishna, G.; Schulte, J.; Cornell, B. A.; Pace, R. J.; Osman, P. D. *Langmuir* . **2003**, *19*, 2294.

(4)   Cornell, B. A. *Opt. Biosens.* **2002**, 457.

(5)   Krishna, G.; Schulte, J.; Cornell, B. A.; Pace, R.; Wieczorek, L.; Osman, P. D. *Langmuir* **2001**, *17*, 4858.

(6)   Raguse, B.; Braach-Maksvytis, V.; Cornell, B. A.; King, L. G.; Osman, P. D. J.; Pace, R. J.; Wieczorek, L. *Langmuir* **1998**, *14*, 648.